Boletim da Sociedade Astronômica Brasileira, **32**, no. 1, 3-9

The impact of stellar activity on orbiting planets

Adriana Valio

[1] Center for Radio Astronomy and Astrophysics Mackenzie, Mackenzie Presbyterian University, Sao Paulo, Brazil
e-mail: avalio@craam.mackenzie.br

Abstract. Stellar activity manifests itself in the form of surface features such as spots and faculae, and flares and mass ejections from its atmosphere. Flares and superflares have been detected from active stars. The impact of the flaring UV flux on possible living organisms in close orbiting planets can be very harmful, however, an atmosphere with ozone could protect them. Mass ejections also affect the planetary atmosphere, being responsible for atmospheric erosion. When an orbiting planet transits in front of the star and occults a spot or a facula, small signatures are imprinted in the transit light curve. These can be modeled to yield the physical characteristics of either spots and faculae, such as size, temperature, location, magnetic field, and lifetime. Monitoring these signatures on multiple transits yields the stellar rotation and differential rotation, and even magnetic cycles for long enough time series.

Resumo. A atividade estelar se manifesta na forma de manchas e faculas na superfície e explosões e ejeções de massa de sua atmosfera. Flares e superflares foram detectadas em estrelas ativas. O impacto do fluxo de radiação UV em possíveis organismos vivos em planetas em uma órbita próxima pode ser muito prejudicial, no entanto, uma atmosfera com ozônio poderia protegê-los. As ejeções de massa também afetam a atmosfera planetária, sendo responsáveis pela erosão atmosférica. Quando um planeta em órbita transita em frente à estrela e oculta uma mancha ou facula, pequenas assinaturas são impressas na curva da luz do trânsito. Estas variações podem ser modeladas inferindo as características físicas de manchas e faculas, como tamanho, temperatura, localização, campo magnético e tempo de vida. O monitoramento destas assinaturas em vários trânsitos determina a rotação estelar e também a rotação diferencial, além ciclos magnéticos no caso de séries temporais de longa duração.

Keywords. Stars: activity – Stars: flare – Stars: magnetic field – Planet-star interactions

1. Introduction

The Sun has been studied over centuries and its spots are well known since ancient times. However with Galileo, spot monitoring entered the modern era with the use of a telescope. In 1843, Schwabe (1843) noticed that the number of sunspots followed a well defined cycle of approximately 11 years (see Figure 1). Not only the number of spots, but also the total irradiance of the Sun presented a periodic variation of only 0.1% that also followed the 11 year periodicity.

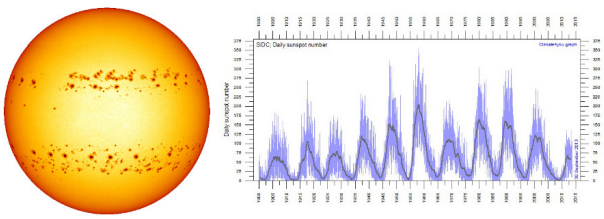

Figure 1. *Left:* Superposed solar image with the spots of one activity cycle. *Right:* Daily sunspot number from 1900 until 2013.

Other stars were later discovered to also exhibit a periodicity in their total flux (see Figure 2. The Mount Wilson HK project, that bears the name of the telescope used in the observations, observed a total of 2300 stars with the goal of inferring their chromospheric activity in Ca II H&K and its variability. This project initiated in 1966 by Wilson Olin, was later continued by Sallie Baliunas and many others until 2002 (Radick et al. 1998). The results showed that the Sun behaved typically as a star of its age and mass. In contrast, young stars were significantly more variable than the present-day Sun. In summary, of the solar-like stars of the Mt. Wilson ample:

- 60% presented periodic activity cycles;
- 15% were variable, without obvious periodicity; and
- 10-15% were non-variable.

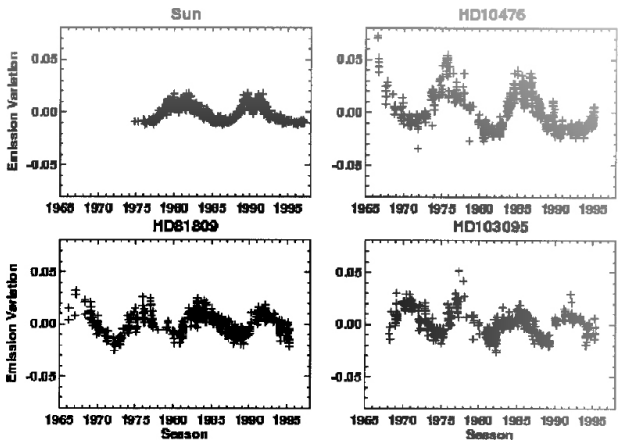

Figure 2. Chromospheric Ca II emission cycles for the Sun and solar–like stars HD 10476, HD 81809, and HD 103095, illustrating the regular cyclic variation that is common in such stars. The Ca II emission is plotted in Mount Wilson "S-Index" units (Radick 2000).

Currently it is known that this activity is driven by a magnetic field generated in the stellar interior by an dynamo mechanism (the $\alpha\Omega$ dynamo) first proposed by Parker (1955). Magnetic activity in solar-type stars declines with age due to a loss of an-

gular momentum caused by a solar like wind throughout the main-sequence lifetime (Skumanich 1972). In solar-type stars, age-activity relation is well defined, with young stars having strong Ca II K line emission with the flux proportional to $t^{-1/2}$, where t is the age of the star (Skumanich 1972). This braking acts until about 2 Gyr (Pace 2013), and is depicted in Figure 3. A 'Skumanich-like' age-activity relation is also found for solar-twins (Lorenzo et al. 2018, see also article by Lorenzo-Oliveira in this volume).

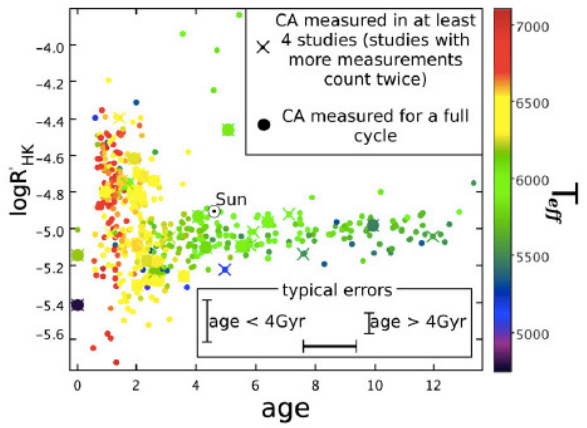

Figure 3. Chromospheric activity index R'HK versus age diagram (Pace 2013).

Stellar activity increases with the size of the convection envelope of the star (West et al. 2004) and rotation rate (West et al. 2015). Most M dwarf stars display significantly enhanced stellar activity when compared to the Sun, and thus M dwarfs do not fit the solar–type relation. Their activity is more prolonged and is a function of both age and mass. Therefore, dMe stars are kinematically younger than dM stars.

2. Spots characterisation

Sunspots were the first indicators of solar activity. Very likely, all cool stars with a convective envelope like the Sun have spots on their surfaces. However, current telescopes do not have the spatial resolution to detect spots similar to sunspots. Nevertheless, there are basically three methods to study starspots: (1) Doppler imaging, (2) photometric modulation, and (3) planetary transit mapping.

Doppler imaging uses the deformations of rotationally–broadened line profiles (see the top panel of Figure 4) to recover the stellar surface temperature distribution (Vogt and Penrod 1983). Therefore, Doppler imaging can only be performed on fast rotating stars. An example of the recovered surface temperature distribution is shown in the bottom panel of Figure 4 for the K0 giant HD 12545 (Strassmeier 1999).

As the star rotates, the presence of dark starspots on its surface will induce periodic photometric variability (Figure 5). This photometric modulation of the stellar light curve can be fit by models to infer the characteristics of these spots (Lanza et al. 2003, 2006, 2009). The first model was applied to the Sun as a star using the SOHO/Virgo data (Lanza et al. 2003). Later this model evolved from a few fixed number of spots on a given time to the Maximum Entropy Method (MEM) where the stellar surface is divided into 200 pixels (Lanza et al. 2009), giving a much better precision of the area coverage of spots.

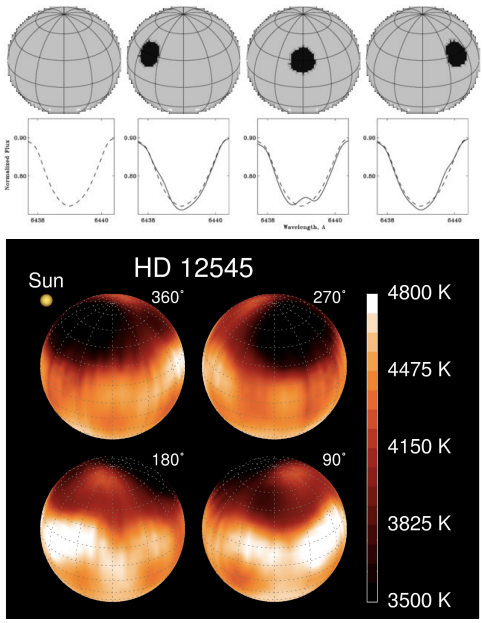

Figure 4. *Top:* Spectral line deformation due to the presence of spots on the visible hemisphere of the star. *Bottom:* Surface temperature distribution map reconstructed from Doppler imaging techniques (Strassmeier 1999).

The last of the three methods, spot transit mapping, was devised by me in 2003 (Silva 2003) and first applied to HD 102458. When a planet transits in front of its host star, there is a chance that it will occult one or more features on the surface of the star, such as dark spots or bright faculae. The type of signature resulting in the transit light curve depends on the spots characteristics and on the planet size. Figure 6 shows the spot signature created when a planet the size of Jupiter (left panel) or Earth (right panel) transits in front of the Sun. Note that a Jupiter sized planet witll cause a transit with 1% decrease in flux, whereas for an Earth planet, the decrease will be only 0.01%, thus the spot signal is relatively larger.

This transit spot model simulates the star as a 2D limb darkened disk, and the planet as a completely dark disk (left panel of Figure 7). The orbit is considered to have zero eccentricity, and at each position of the planet on its orbit, the sum of all the pixels in the image yields each data point of the light curve. This

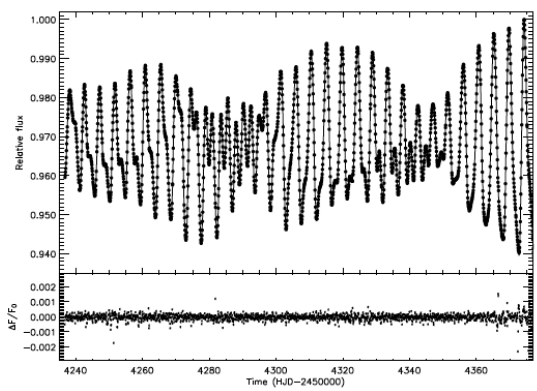

Figure 5. *Top:* Out–of–transit observations of CoRoT-2 (filled dots) versus time with the best fit obtained with the ME model including only cool spots (solid line). *Bottom:* Residuals of the best fit in relative flux units versus time (Lanza et al. 2009).

model allows for the insertion of dark or bright features on the surface of the star, with a given size and intensity. Thus the fit of the transit light curve by this model with a certain number of spots allows the characterisation of the spots physical parameters. This methodology has already been applied to HD 209458 (Silva 2003), CoRoT-2 (Silva-Valio et al. 2010; Silva-Valio & Lanza 2011), Kepler-17 (Valio et al. 2017), Kepler-71 (Zaleski et al. 2019), and Kepler-63 (Netto & Valio 2020). Since then, many models of starspot transit have been developed, for example: PRISM: Tregloan-Reed et al. (2013, 2015, 2018); SOAP-T: Oshagh et al. (2013); spotrod: Béky et al. (2014); KSint: Montalto et al. (2014); ellc: Maxted (2016); StarSim: Herrero et al. (2016); and PyTranSpot: Juvan et al. (2018).

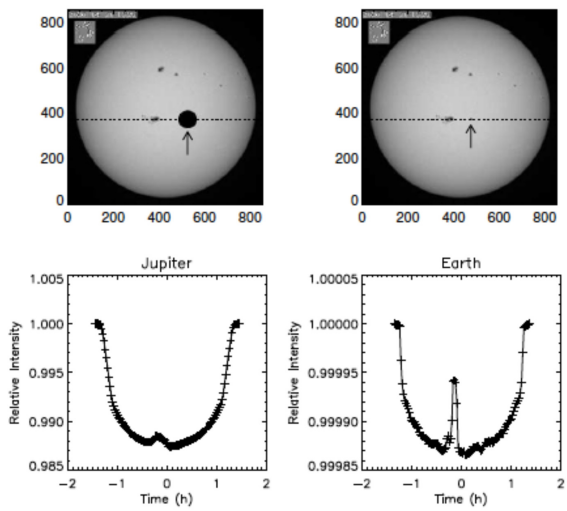

Figure 6. Solar image with transit simulations in front of a spot from a Jupiter (left) and Earth (right) sized planet (Silva-Valio 2009).

The transit light curve fit by the Silva (2003) model yields the size, intensity or temperature, location on the stellar disk of spots. In the case depicted in Figure 7 for the modelling of the 100th transit of Kepler-17b (Valio et al. 2017), three spots are evident. Even though Kepler-17 is a solar–like star (T_{eff} = 5780 K) despite being much younger than the Sun, these three spots are about 7 times larger and slightly warmer than sunspots.

3. Stellar rotation

Another important factor to stellar activity is stellar rotation, since rotation is believed to be a key ingredient in dynamo mechanisms. A survey of stellar rotation found that 25% of stars have rotation rates above 2 km/sec. Nielsen et al. (2013) analysed 12,151 stars from Kepler lightcurves, computing the Lomb-Scargle periodogram for individual quarters of every star (Figure 8). Periods between 1 and 100 days were determined. Later type dwarfs are more likely to have measurable rotation because rotation takes longer to decay in the later M dwarfs. However, there is no strong correlation between activity level and the rate of rotation in these low mass stars. Among very late M dwarfs, some rapid rotators do not show activity. Thus, a low threshold for rotation is needed to maintain activity in M dwarfs.

Silva-Valio (2008) showed that the transit mapping method also provides rotation period and even differential rotation can be estimated. These calculations are based on the assumption that the same spot can be detected on a later transit after a considerable rotation of the star.

4. Magnetic field and magnetic cycles

From a study of 32,317 sunspots from 6970 SOHO/MDI images and magnetograms of the Sun taken during Cycle 23 (1996-2008), Valio et al. (2020) obtained relations between the physical parameters of sunspots. An interesting relation is that between sunspot intensity, I_{spot}, and its maximum magnetic field in Gauss:

$$B_{mag} = (4848 \pm 15) - (4008 \pm 20)\frac{I_{spot}}{I_{star}} \quad (1)$$

If this same relation is valid for solar–like stars, such as CoRoT-2, Kepler-17, Kepler-63, and Kepler-71, we find magnetic fields that are about twice as strong as those on the Sun. The younger the star, the stronger the magnetic field.

Short magnetic activity cycles may also be investigated by analysing the 4 yr Kepler light curves of spotted stars. Estrela & Valio (2016) basically counted the spots on the surface of Kepler-17 and Kepler-63 within the planetary transit band during the 4 years of observations. Periods of about $P_{cycle} = 1.12 \pm 0.16$ year (Kepler-17) and $P_{cycle} = 1.27 \pm 0.16$ year (Kepler-63) were determined. These short cycles may be the analogues of the quasi–biennial oscillations (QBOs) also present in the Sun. Due to the short duration of the observations, it is not possible to detect longer magnetic cycles such as the solar one of 11 years.

5. Stellar activity impact

When radiation and particles produced by solar activity reach the Earth, they may cause: lethal doses of X ray radiation to astronauts; alteration in satellite orbits; geomagnetic storms; ionospheric alterations; affect long distance communications; current peaks in transmission lines; blackouts; erratic behaviour of navigation instruments; ozone layer alterations; and the beautiful display of auroras. Still controversial is the influence of solar activity on Earth's climate. Also hazardous to orbiting planets is the activity of their host star in the form of flares and coronal mass ejections. Moreover, the stellar wind may severely impact the atmosphere of exoplanets that are too close to the star or do not have a magnetosphere.

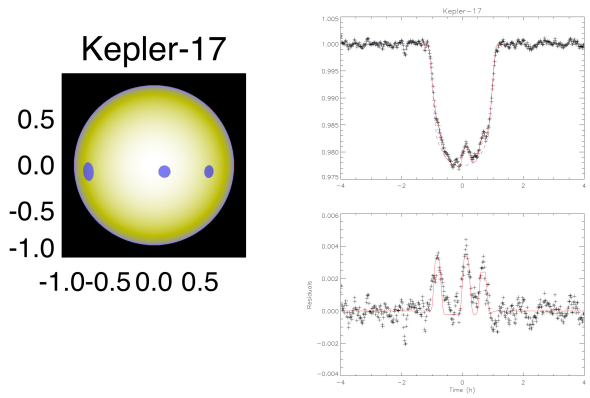

Figure 7. The 100th transit of Kepler-17b. *Left:* Synthesised star with three spots. *Top right:* Transit light curve with superposed model of a spotless star (blue) and a star with three spots (red curve). *Bottom right:* Residuals of the transit light curve after subtraction of a spotless star model. The red curve shows the fit to the data "bumps" (Valio et al. 2017).

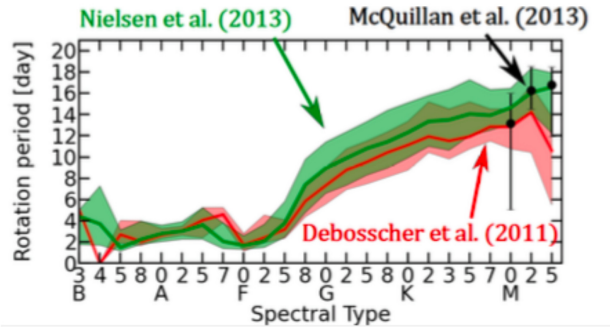

Figure 8. Rotation periods of the stars, averaged within each spectral type. Also shown is the median of the rotation periods measured by McQuillan et al. (2013) (black points with errorbars). Similarly, the red curve shows the median of the rotation periods found by Debosscher et al. (2011). Shaded areas and error bars span the upper and lower 34th percentile values from the median (Nielsen et al. 2013).

5.1. Stellar winds and coronal mass ejections

Stellar winds may cause erosion of the orbiting planets atmosphere if this planet does not have a protective magnetic field. This is believed to be what happened to Mars in the past when it had running water on its surface, probably maintained by an atmosphere that was later lost. Coronal mass ejections will further contribute to the loss of a planetary atmosphere. Ultraviolet radiation from young stars and flaring activity induce the photoevaporation of atmospheric gases therefore precluding the habitability of surrounding planets, specially those in close–in orbits.

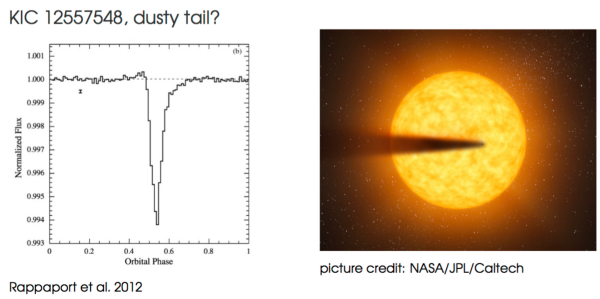

Figure 9. *Left:* Folded light curves of KIC 12557548 (Rappaport et al. 2012). Short illustrative vertical bar on the left is the standard error of the data points within a bin. *Right:* Artist conception of an evaporating planet.

An artist conception of an evaporating exoplanet is shown in the right panel of Figure 9, whereas the left panet shows the actual transit of KIC 12557548b, which distortion is interpreted as due to a comet–like tail of the evaporating planet atmosphere (Rappaport et al. 2012). This scenario is what is expected for planets too close to their stars. Kislyakova et al. (2013) investigated the interactions between the stellar wind of a typical M star and the hydrogen-rich upper atmospheres of an Earth-like and a super–Earth planets within the habitable zone (approximately at 0.24 AU). The formation and evolution of an extended atmosphere was studied depending on the stellar soft-ray and UV fluxes, characteristics of the stellar wind such as density and velocity, if the planet had or not a magnetosphere, and the loss of planetary atmosphere due to pick-up ions.

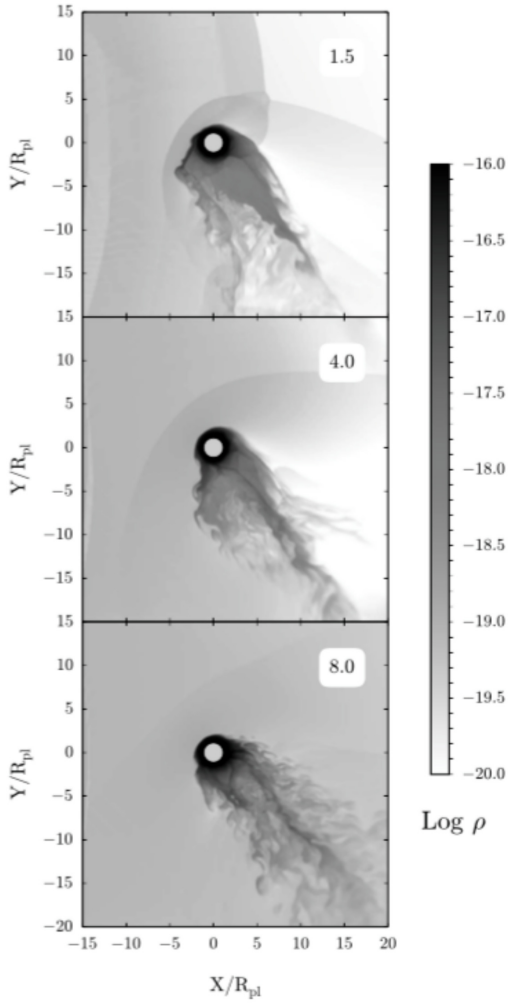

Figure 10. Distribution of the density in a closed exoplanet envelope subject to the action of a CME, for various moments in time. The star is located to the left and the white circle at the centre represents the planet. The time in hours measured from the onset is given in the upper right corner of each diagram (Bisikalo & Cherenkov 2016).

Bisikalo & Cherenkov (2016) performed 3D MHD simulation of the passage of a coronal mass ejection (CME) through a hot Jupiter. The wind was of solar–type as well as the CME. The authors found that the CME was sufficient to tear off the outer part of the planet envelope beyond the Roche lobe and carry it away from the exoplanet (see Figure 10).

5.2. Flares and biological impact

The Kepler satellite monitored continuously over 160,000 stars (Borucki et al. 2010). Sudden increase in the brightness of a star indicate flaring activity such as the ones depicted in Figure 11 (Maehara et al. 2012). These flares are much more powerful than solar flares ($E < 10^{32}$ erg), reaching energies of 1000 to 10,000 times larger. Superflares on 9751 solar–type stars were studied by Maehara et al. (2012), which analysed 365 superflares with energy $> 10^{35}$ ergs in 148 stars. Late M dwarfs have a flaring frequency 1000 times larger than the the Sun.

These superflares release significant amounts of X-rays, EUV, and UV radiation. Depending on the energy of the flare, they can cause changes in the planetary atmosphere such as atmospheric loss by photoevaporation and alter the chemical com-

position of the upper atmosphere. Also the protons from the flare produce odd nitrogen and odd hydrogen in the upper stratosphere and mesosphere that destroy the ozone (Segura et al. 2010). This could affect the origin and evolution of life.

With the goal of determining if the superflares can be dangerous to life present in the surface/ocean of planets, Estrela & Valio (2018) analysed the effect of the UV flare radiation on a hypothetical Earth–like planet orbiting Kepler-96 at 1 AU, and on the three planets in the habitable zone of TRAPPIST-1. The habitable zone (HZ) is a region from the star comprised between the temperature limits where water would stay in the liquid state on the surface of a terrestrial planet.

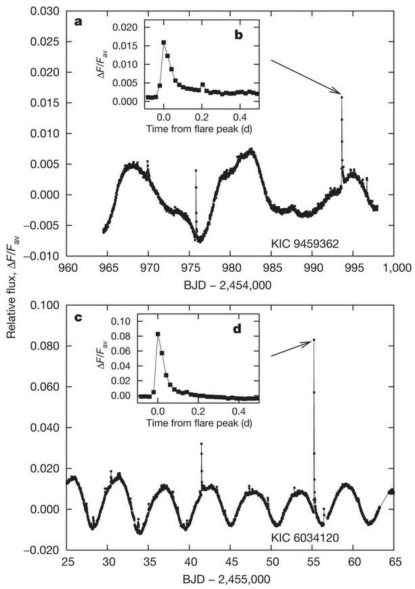

Figure 11. Light curve of typical superflares on solar-type stars (Maehara et al. 2012).

Kepler-96 is an interesting target because it is solar–like and has an age that corresponds to the end of the Archean Era on Earth, when the Great Oxygenation Event took place. This fresh and abundant supply of oxygen is believed to have favoured the development of multicellular organisms here on Earth. Since the young Sun was fainter, the emission at the top of the atmosphere was considered to be 75% of the present-day solar irradiation.

Three superflares were observed during transits of Kepler-96b, a Super–Earth too close to the star, and more flares were detected in the light curve of Kepler-96 during the 4 years of observation. The larger of these flares (left panel of Figure 12) had an energy of 1.8×10^{35} ergs. Two model atmospheres were considered for the hypothetical Earth at 1AU: (1) Archean (3.9 Gyr – 2.5 Gyr) with 80% N_2 and 20% CO_2 and (2) Present day, with 80% N_2 and 20% O_2.

Superflares can increase the UV flux emitted by the star during a short period of time. As a proxy to estimate the total UV flux radiated during theses superflares, the strongest solar flare recorded in history, an X17 flare that occurred on October 28th, 2003 (Woods et al. 2004), was considered. The UV flux of this flares amounted to 12% of the total flux of the flare (4×10^{32} erg). A simple proportionality between the solar and Kepler-96 flares yields that the superflare increased the amount of UV radiation reaching the planet by 5400%.

If a planet has an atmosphere with absorbers such as N_2, CO_2, or O_2, the short wavelengths (0.1-200nm) UV radiation is attenuated at the top of the atmosphere. The UVB and UVC

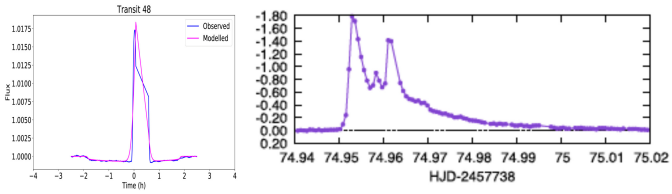

Figure 12. *Left:* Strongest flare of Kepler-96 observed during the 48th transit of the Super Earth Kepler-96b (Estrela & Valio 2018). *Left:* Strongest flare from TRAPPIST-1 observed during the K2 mission (Vida et al. 2017).

flux can be attenuated by an ozone layer. However, for a depleted or non existent ozone layer, the DNA is mainly damaged by radiation in the UVC and UVB range (200-300nm). The response of a biological body depends on the wavelength and duration of exposure. Therefore, it is necessary to weight the incident flux by the action spectra, a function that expresses the biological response effectiveness at different wavelengths. Estrela & Valio (2018) considered the action spectrum of two bacteria: *Escherichia coli* and *Deinococcus radiodurans*. The latter an extremophile that can survive in extreme environment conditions such as vacuum, dehydration, and high dosages of UV radiation. The maximum flux dosage for 10% survival is 22.5 and 553 J/m^2 for *E. coli* and *D. radiodurans*, respectively.

The result of the biological effectiveness fluence calculation showed that, in the event of a superflare, *E. coli* and *D. radiodurans* would only survive on the surface of the hypothetical Earth in orbit of Kepler-96 at 1AU if an ozone layer was present in the planet atmosphere. However, not only superflares but other stellar magnetic activity phenomena, such as CMEs, could cause a significant depletion of the ozone layer, even strip away its atmosphere.

An ocean on a planet in the habitable zone of the star could protect living organisms from the increased UV radiation due to the superflares therefore allowing life to thrive in depths within the photic zone (up to 200 m), as in Earth's case. Therefore, we analysed if an ocean could preserve living beings from the harshness of superflares. The answer is yes for depths of 28m for *E. coli* and only 12m for *D. radiodurans* (Estrela & Valio 2018).

The same calculation was performed for the 3 planets in the habitable zone of the M dwarf TRAPPIST-1. This star is very active, with 47 flares detected with energies between 10^{30} and 10^{33} ergs (Vida et al. 2017). The largest flare released a total energy of 1.24×10^{33} erg over 43 min (see right panel of Figure 12). The UV flux contribution from TRAPPIST-1, was taken as the same UV flux measured from flares of Ad Leo, also an M red dwarf (Hawley & Pettersen 1991), whereas the atmosphere model was taken from O'Malley & Kaltenegger (2017). The result was similar to the one for the hypothetical Earth around Kepler-96. Bacteria such as *E. coli* and *D. radiodurans* could only survive on the surface of the TRAPPIST-1 planets in the HZ if there was an ozone layer present in their atmospheres, or in shallow waters of an ocean (Valio et al. 2019).

6. Summary and conclusions

Living around an active star can be very hazardous mainly due to stellar winds, superflares, and coronal mass ejections. These active phenomena can strip away the planetary atmosphere or impinge lethal dosages of X-ray and UV radiation. The presence of a magnetosphere can help prevent atmospheric loss of a

planet. Neverhteless, the impact of the UV radiation produced in superflares can be estimated as shown by Estrela & Valio (2018); Valio et al. (2019).

Thus, characterising stellar activity is paramount to understanding the space weather of the orbiting planets. One way to due this is by modelling the small variations observed in the transit light curves believed to be caused by spots or faculae on the stellar surface. The first planetary transit modelling of spots was developed by Silva (2003). This transiting mapping model yields:

1. **Spots physical characteristics**: size, temperature, location – active longitudes, evolution/lifetime, surface area coverage (Silva 2003);
2. **Stellar rotation period** (Silva-Valio 2008) in the case of multiple transits of the same feature, as well as
3. **Stellar differential rotation** (Silva-Valio et al. 2010; Silva-Valio & Lanza 2011; Valio et al. 2017; Zaleski et al. 2019);
4. **Stellar activity cycles** (Estrela & Valio 2016) for longer observing periods (> 1yr).

Acknowledgements. The partial financial support of FAPESP and CNPq for my research throughout the years is greatly appreciated, as well as the fellowships from FAPESP, CNPq, and CAPES of my undergraduate and graduate students.

References

Béky, B., Kipping, D. M., & Holman, M. J. 2014, "SPOTROD: a semi-analytic model for transits of spotted stars", MNRAS, 442: 3686-3699

Bisikalo, D. V. & Cherenkov, A. A. 2016, "The influence of coronal mass ejections on the gas dynamics of the atmosphere of a "hot Jupiter" exoplanet", ARep, 60: 183-192

Borucki, W. J., Koch, D., Basri, G. 2010, "Kepler Planet-Detection Mission: Introduction and First Results", Science, 327: 977-980

Debosscher, J., Blomme, J., Aerts, C., & De Ridder, J. 2011, "Global stellar variability study in the field-of-view of the Kepler satellite", A&A, 529: 89-103

Estrela, R. & Valio, A. 2016, "Stellar Magnetic Cycles in the Solar-like Stars Kepler-17 and Kepler-63", ApJ, 831: 57-68

Estrela, R. & Valio, A. 2018, "Superflare Ultraviolet Impact on Kepler-96 System: A Glimpse of Habitability When the Ozone Layer First Formed on Earth", AsBio, 18: 1414–1424

Hawley, S. L., & Pettersen, B. R. 1991, "The Great Flare of 1985 April 12 on AD Leonis", ApJ378: 725-741

Herrero, E., Ribas, I., Jordi, C., et al. 2016, "Modelling the photosphere of active stars for planet detection and characterization", A&A, 586: 131-149

Juvan, I. G., Lendl, M., Cubillos, P. E., Fossati, L., Tregloan-Reed, J., Lammer, H., Guenther, E. W., Hanslmeier, A., 2018, "PyTranSpot: A tool for multiband light curve modeling of planetary transits and stellar spots", A&A, 610, 15-31

Kislyakova, K. G., Lammer, H., Holmström, M., Panchenko, M., Odert, P., Erkaev, N. V., Leitzinger, M., Khodachenko, M. L.; Kulikov, Y. N., Güdel, M., Hanslmeier, A. 2013, "XUV-Exposed, Non-Hydrostatic Hydrogen-Rich Upper Atmospheres of Terrestrial Planets. Part II: Hydrogen Coronae and Ion Escape", AsBio, 13: 1030–1048

Lanza, A. F., Rodonò, M., Pagano, I., Barge, P., Llebaria, A. 2003, "Modelling the rotational modulation of the Sun as a star", A&A, 403: 1135-1149

Lanza, A. F., Messina, S., Pagano, I., Rodonò, M. 2006, "A model to simulate synthetic light curves of solar-like stars", AN, 327: 21

Lanza, A. F., Pagano, I., Leto, G., Messina, S., Aigrain, S., Alonso, R., Auvergne, M., Baglin, A., Barge, P., Bonomo, A. S., Boumier, P., Collier Cameron, A., Comparato, M., Cutispoto, G., de Medeiros, J. R., Foing, B., Kaiser, A., Moutou, C., Parihar, P. S., Silva-Valio, A., Weiss, W. W. 2009, "Magnetic activity in the photosphere of CoRoT-Exo-2a. Active longitudes and short-term spot cycle in a young Sun-like star", A&A, 493: 193–200

Lorenzo-Oliveira, D., Freitas, F. C., Meléndez, J.; Bedell, M., Ramírez, I., Bean, J. L.; Asplund, M., Spina, L., Dreizler, S., Alves-Brito, A., Casagrande, L. 2018, "The Solar Twin Planet Search. The age-chromospheric activity relation", A&A, 619: 73-86

Maehara, H., Shibayama, T., Notsu, S., et al. 2012, "Superflares on solar-type stars", Nature, 485: 478

McQuillan, A., Aigrain, S., & Mazeh, T. 2013, "Measuring the rotation period distribution of field M dwarfs with Kepler", MNRAS, 432: 1203–1216

Maxted, P. F. L. 2016, "ellc: A fast, flexible light curve model for detached eclipsing binary stars and transiting exoplanets", A&A, 591: 111-126

Montalto, M., Boué, G., Oshagh, M., et al. 2014, "Improvements on analytic modelling of stellar spots", MNRAS, 444: 1721–1728

Nielsen, M. B., Gizon, L., Schunker, H. & Karoff, C. 2013, "Rotation periods of 12 000 main-sequence Kepler stars: Dependence on stellar spectral type and comparison with v sin i observations", A&A, 557: L10-L13

Netto, Y. & Valio, A. 2020, "Stellar Magnetic Activity and "Butterfly Diagram" of Kepler-63", A&A(accepted)

O'Malley, J. T. & Kaltenegger, L. 2017, "UV surface habitability of the TRAPPIST-1 system", MNRAS, 469: L26-30

Oshagh, M., Boisse, I., Boué, G., Montalto, M., Santos, N. C., Bonfils, X., Haghighipour, N. 2013, "SOAP-T: a tool to study the light curve and radial velocity of a system with a transiting planet and a rotating spotted star", A&A, 549: 35-42

Pace, G. 2013, "Chromospheric activity as age indicator. An L-shaped chromospheric–activity versus age diagram", A&A, 551: L8-L11

Parker, E. N. 1955, "Hydromagnetic Dynamo Models", ApJ, 122: 293:314

Radick, R. R., Lockwood, G. W., Skiff, B. A., & Baliunas, S. L. 1998, "Patterns of variation among Sun-like stars" ApJS, 118: 239-258

Radick, R. R. 2000, "A brief survey of chromospheric and photometric variability among sunlike stars", Adv. Space Res., 26: 1739-1745

Rappaport, S., Levine, A., Chiang, E., El Mellah, I., Jenkins, J., Kalomeni, B., Kite, E. S., Kotson, M., Nelson, L., Rousseau-Nepton, L., Tran, K. 2012, "Possible Disintegrating Short-period Super-Mercury Orbiting KIC 12557548", ApJ, 752: 1-13

Schwabe, S. H. 1843, "Sonnenbeobachtungen im Jahre 1843" [Observations of the sun in the year 1843]. Astronomische Nachrichten [Astronomical News] (in German), 21: 233–236

Segura, A., Walkowicz, L. M., Meadows, V., Kasting, J., Hawley, S. 2010, "The Effect of a Strong Stellar Flare on the Atmospheric Chemistry of an Earth-like Planet Orbiting an M Dwarf", AsBio, 10: 751–771

Silva, A. V. R. 2003, "Method for spot detection on solar–like stars", ApJ, 585, L147–L150

Silva-Valio, A. 2008, "Estimating stellar rotation from starspot detection during planetary transits", ApJ, 683: L179–L182

Silva-Valio, A. 2009, "Starspot detection from planetary transits observed by CoRoT", R.Mex. A. Conference Series, 35: 13-18

Silva-Valio, A., Lanza, A. F., Alonso, R., & Barge, P. 2010, "Properties of starspots on CoRoT-2", A&A, 510: 25-30

Silva-Valio, A., & Lanza, A. F. 2011, "Time evolution and rotation of starspots on CoRoT-2 from the modelling of transit photometry", A&A, 529: 36-45

Skumanich, A. 1972, "Time Scales for CA II Emission Decay, Rotational Braking, and Lithium Depletion", ApJ, 171: 565-567

Strassmeier, K. G. 1999, "Doppler imaging of stellar surface structure. XI. The super starspots on the K0 giant HD 12545: larger than the entire Sun", A&A, 347: 225-234

Tregloan-Reed, J., Southworth, J., & Tappert, C. 2013, "Transits and starspots in the WASP-19 planetary system", MNRAS, 428: 3671–3679

Tregloan-Reed, J., Southworth, J., Burgdorf, M., et al. 2015, "Transits and starspots in the WASP-6 planetary system", MNRAS, 450: 1760–1769

Tregloan-Reed, J., Southworth, J., Mancini, L., Mollière, P., Ciceri, S., Bruni, I., Ricci, D,; Ayala-Loera, C., Henning, T. 2018, "Possible detection of a bimodal cloud distribution in the atmosphere of HAT-P-32 A b from multiband photometry", MNRAS, 474: 5485–5499

Valio, A. 2013, New Quests in Stellar Astrophysics III: A Panchromatic View of Solar-Like Stars, With and Without Planets, 472, 239

Valio, A., Estrela, R., Netto, Y., et al. 2017, "Activity and Rotation of Kepler-17", ApJ, 835: 294-299

Valio, A., Estrela, R., Cabral, L. & Grangeiro, A. 2019,"The biological impact of superflares on planets in the Habitable Zone", In "Origins: From the Protosun to the First Steps of Life", Proceedings IAU Symposium No. 345

Valio, A., Spagiari, E., Marengoni, M., & Selhorst, C. 2020, "Correlations of sunspots physical characteristics during cycle 23", Sol. Phys.(submitted)

Vida, K, Kovari, Zs., Pal, A., K. Olah, K, & Kriskovics, L. 2017, "Frequent Flaring in the TRAPPIST-1 System – Unsuited for Life?", ApJ, 841: 124-129

Vogt, S. S.; Penrod, G. D. 1983, "Doppler imaging of spotted stars : application to the RS Canum Venaticorum star HR 1099", PASP, 95: 565-576

West, A. A., Hawley, S. L., Walkowicz, et al. 2004, "Spectroscopic Properties of Cool Stars in the Sloan Digital Sky Survey: An Analysis of Magnetic Activity and a Search for Subdwarfs", AJ, 128:426

West, A. A., Weisenburger, K. L., Irwin, J., Berta-Thompson, Z. K., Charbonneau, D., Dittmann, J., Pineda, J. S. 2015, "An Activity–Rotation Relationship and Kinematic Analysis of Nearby Mid-to-Late-Type M Dwarfs", ApJ, 812: 3-14

Woods, T.N., Eparvier, F.G., Fontenla, J., et al. 2004, "Solar irradiance variability during the October 2003 solar storm period", Geophys Res Lett 31: L10802.

Zaleski, S. M., Valio, A., Marsden, S. C., Carter, B. D. 2019, "Differential rotation of Kepler-71 via transit photometry mapping of faculae and starspots", MNRAS, 484, 618